DOI: 10.1002/adsc.201((will be filled in by the editorial staff))

Graphene-Supported, Well-Defined Metal-Based Catalysts for C-H Bond Functionalization and Related Reactions

Jonathan Martínez-Laguna,[a] Ana Caballero*,[a] and Pedro J. Pérez*,[a]

[a]Laboratorio de Catálisis Homogénea, Unidad Asociada al CSIC, CIQSO-Centro de Investigación en Química Sostenible and Departamento de Química, Universidad de Huelva, Campus de El Carmen s/n, 21007-Huelva, Spain
e-mail: perez@dqcm.uhu.es, ana.caballero@dqcm.uhu.es

Abstract. The use of graphenic materials as support for transition metal-based catalysts in reactions involving the functionalization of carbon-hydrogen bonds is reviewed. In many cases, the catalytic activities reported are comparable or better than the homogeneous counterparts, a feature which adds to a substantial degree of recyclability of the materials.

Keywords: C–H functionalization, graphene anchoring, graphenic supports, heterogeneous catalysis, supported metal complexes

1. Introduction

Homogeneous catalysis employing soluble transition metal complexes has led to a large number of highly efficient synthetic procedures with particular success in terms of chemo-, regio-, enantio- or diastereo- selectivities.[1] The homogeneous-heterogeneous comparisons historically comprised the dichotomy of the higher selectivity in the former and the better performance in terms of stability and catalyst separation of the latter.[2] Along the years, the development of more stable transition metal complexes as catalysts capable of surviving drastic reaction conditions has left catalyst separation (and its subsequent reuse) as the main drawback to circumvent within the homogeneous catalysis field. A general strategy toward that end consists in the conversion of a successful homogeneous catalyst into a heterogeneous catalytic system upon its anchoring onto a solid support,[3] which generally is inert toward the pursued reaction, in such a way that the catalytic behaviour in solution in maintained in the insoluble supported catalyst.

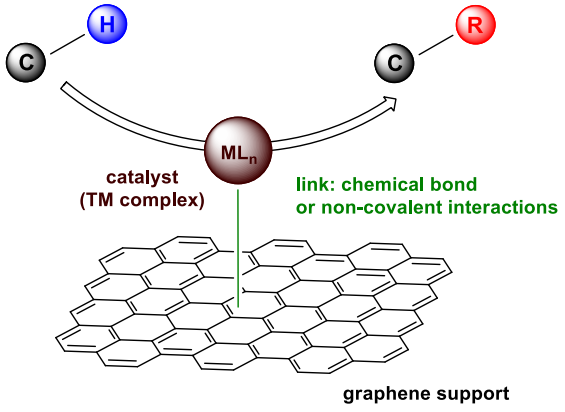

Scheme 1. Graphene-supported well-defined transition metal complexes as catalysts for C–H bond functionalization reactions.

The above common tactic has been developed using an inorganic solid, such as silica, zeolites, or metal oxides, among others, either through chemical bonding or physical forces. Many of those supports

[a] J. Martínez-Laguna, Dr. A. Caballero, Prof. Dr. P. J. Pérez
Laboratorio de Catálisis Homogénea, Unidad Asociada al CSIC
CIQSO-Centro de Investigación en Química Sostenible and Departamento de Química
Universidad de Huelva, 21007-Huelva (Spain)
The ORCID identification numbers) for the authors of this article can be found under https://doi.org/10.1002/chem.2018XXXXXt.

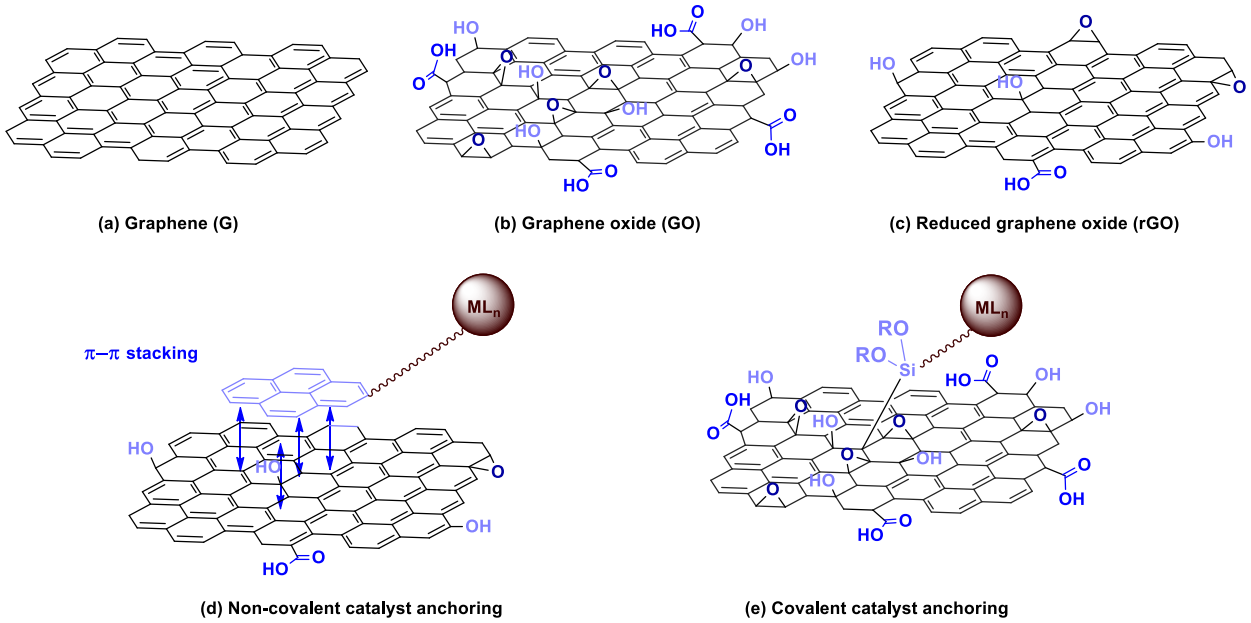

Scheme 2. Graphene materials employed as catalyst supports and examples of catalyst anchoring strategies.

contain a porous surface,[4] and a fraction of the active sites is located inside them. Thus, the diffusion of reactants and products in and out of the pores, respectively, may exert a certain influence in the reaction kinetics. The use of high surface area materials and low porosity can enhance the catalyst performance. This is the origin of the recent use of carbon nanomaterials, displaying a large surface area,[5] as catalyst supports. Until the isolation of graphene (G) in 2004,[6] graphite, diamond, fullerenes and carbon nanotubes were explored as supports. Graphene brought a substantial change to the field, [7], since the specific surface area of fully exfoliated G displays the largest values for carbon-based supports.[8] Consequently, this feature allows interactions without restrictions of the supported units with the components in the reaction mixture.

In this contribution, we aim at providing an overview of the use of graphene materials as support for well-defined catalysts, [9] based on transition metal (TM) complexes, in reactions involving carbon-hydrogen bond functionalization processes (Scheme 1). In addition to the catalytic reaction *per se*, the advantages of using graphene supports will be highlighted, showing the potential of such solid not only from the mere point of view of catalyst separation but also being non-innocent toward the catalytic behaviour.

2. Types of Graphene-based materials (Gs) as supports.

Graphene (G, Scheme 2a) is an allotrope of carbon composed of a hexagonal network with honeycomb structure consisting of sp^2-hybridized carbon atoms bonded in a two-dimensional (2D) planar surface. One of the most remarkable characteristics is that the degree of atom utilization in graphene is very high, and the largest possible among all the inorganic solids, since in most of the latter only the superficial atoms are accessible for linkage, small pores being very often useless for catalyst anchoring.[10] At variance, the two-dimensional nature of graphene sheets makes most of the surface available for the attaching.

There are several types of functionalized graphenes[7a,11] such graphene oxide (GO, Scheme 2b), reduced graphene oxide (rGO, Scheme 2c), graphene acid (GA), graphitic carbon nitride and graphdiyne or graphyne, which have been used as supports with anchored transition metal complexes as catalysts, albeit G, GO and rGO are, by far, the most frequently employed.

Surface chemical properties of graphene must be mentioned as they are crucial for catalyst anchoring as well as, in some cases, for explaining the catalytic behaviour of a graphene-supported catalyst. The sp^2 hybridization of carbon atoms and the extended molecular π orbital makes G able to interact with certain molecules not only by van der Waals forces, but also by stronger π–π interactions. These non-covalent interactions are located on the graphene layers, whereas covalent interactions require the existence of defects (intrinsic or induced by surface doping or modification) on graphene structure.[12]

Jonathan Martinez-Laguna is currently at the Graduate School at Universidad de Huelva, under the supervision of Dr. Ana Caballero and Prof. Pedro J. Pérez. He graduated in Chemistry (Bs.C.) at Universidad de Salamanca (2018) and later obtained his Master Degree at Universidad de Valladolid (2019), his Master Thesis being carried out in palladium chemistry under the supervision of Prof. Pablo Espinet.

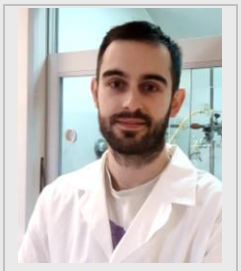

Ana Caballero is Senior Lecturer in Inorganic Chemistry at Universidad de Huelva, Spain. She graduated in Chemistry at the Universidad de Sevilla (1999) and obtained her PhD from the Universidad de Huelva under the supervision of Prof. Pedro J. Pérez (2004). Later she moved to the LCC (CNRS, Toulouse) for a postdoctoral stay with Prof. Sylviane Sabo-Etienne. She returned (2007) to the Universidad de Huelva as a ''Ramon y Cajal'' Postdoctoral Associate, to become first Lecturer and currently Senior Lecturer. In the recent years she has focused on the development of the catalytic functionalization of methane based on the use of supercritical fluids as reaction medium.

Pedro J. Pérez (FRSC, CE Fellow) is Professor of Inorganic Chemistry at Universidad de Huelva, Spain, where he joined in 1993 after obtaining his Ph. D. Degree at Universidad de Sevilla (1991, Ernesto Carmona, Advisor) and postdoctoral stay at University of North Carolina, Chapel Hill (1991-1993, Maurice Brookhart, spupervisor). His work is mainly devoted to the development of late transition-metal complexes as catalysts for transformations involving saturated and unsaturated hydrocarbons. He is the founder of the Center for Research in Sustainable Chemistry (CIQSO) at Universidad de Huelva, where he is the Leader of the Homogeneous Catalysis Laboratory.

Non-covalent immobilization of coordination complexes has been less studied than strategies involving covalent bonding since strong interactions between the anchored unit and the graphene surface are preferred in order to avoid significant catalyst leaching. However, this methodology represents an attractive approach since it requires few synthetic efforts and does not change neither the catalyst molecular structure nor the electronic properties of graphene. The use of pyrene ponytails[13] at a position far from the metal centre is, to date, the most employed polyaromatic system to perform π–π stacking with graphene (Scheme 2d). In addition to pyrene, other aromatic systems like porphyrin, anthracene, phenanthroline, naphthalene or cyclopentadienyl rings have been used for non-covalent immobilization.[14]

On the other hand, processes toward covalent anchoring of metal complexes on graphenic materials require more efforts from a synthetic point of view. This approach may increment catalyst stability with respect to the use of non-covalent strategies. The most common reason for deactivation of a covalently anchored catalyst is degradation of the ligand (a silane-containing bridge in the example shown in Scheme 2e) under the reaction conditions. Covalent anchoring ensures that no desorption of the covalently attached molecule from the support will occur, which is a potential drawback when non-covalent anchoring is employed.[15]

The type of graphene-based material chosen as a support depends on the application of the anchored catalytic species. For catalytic applications GO or rGO have been widely used as starting materials to anchor metal complexes. Graphene oxide[16] (Scheme 2b) is decorated with a wide range of functional groups containing oxygen (such as alcohols, epoxides and carboxylic acids) and topological defects which can be used as anchoring centres for the metallic complex. GO is typically prepared by the reaction between graphite and strong oxidants under acidic conditions. The advantages of using GO as a support instead of graphene can be summarized as follows:[17] (1) graphene oxide is more readily available and cheaper; (2) the amphiphilic nature and excellent dispersibility of GO in both aqueous and organic solvents render the surface more accessible; (3) the binding energy of the oxygen-doped surface of graphene oxide is significantly higher; and (4) the covalent immobilization of catalytically active species can be easily achieved by surface functionalization.

Most of the examples of covalent functionalization of GO takes advantage of the use of alkoxy silanes. This can be performed either through a pre-functionalization of GO surface by reaction between alkoxy silanes and hydroxyl groups followed by incorporation of the catalysts or the direct incorporation of silane-containing catalysts to the GO material, the final result being the linkage of the catalyst to the surface via a silanoxy fragment.[18] Besides the functionalization of GO via hydroxyl groups, processes such as silylation, esterification and amidation reactions of carboxyl groups have been performed to create a covalent bond between the support and the ligand or the complex. Also, carboxylate groups may act as ligands for the direct immobilization of complexes via coordination to the metal centre whereas the reactivity of epoxy groups can be employed to build a covalent bond.

Reduced-graphene oxide (rGO) is prepared[19] by GO reduction (thermal/H_2, electrochemical or chemical reactions) which partially restores the structure and properties of G with the reintroduction of large aromatic domains upon removal of some oxygenated functional groups. Apart from the synthetic procedure employed, in all cases rGO contains residual oxygen groups, as well as structural defects.[20] It serves as support for transition metal

complexes with catalytic properties following the aforementioned strategies, preferentially using the non-covalent anchoring via π–π stacking and van der Waals interactions.

3. Carbon-hydrogen bond catalytic functionalization with graphene-supported well-defined catalysts.

This section is organized according to the type of the catalytic reaction, always under the premise that a C–H bond of the substrate is activated/functionalized. Examples in which graphene-supported TM catalysts induce transformations not involving such C–H bond modification are not considered herein. The first section is devoted to cross-coupling reactions, and is followed by oxidation processes, three-component reactions and miscellaneous examples.

The linkages of the metal complexes to the graphene-derivative surface are defined in the drawings by colouring the linkers, albeit the exact position of the surface at which they are connected are, in most cases, unreported.

It is also worth mentioning that when turnover numbers (mol product / mol catalyst, TON) or turnover frequencies (mol product / mol catalyst x time, TOF) are provided, they are referred to the total equiv of the metal catalyst supported, which are previously determined by spectroscopic data. Usually it is assumed that all them are active in catalysis.

3. 1. Cross-coupling reactions.

Cross-coupling reactions[21] represents a class of reactions where a C–C, C–H, C–N, C–O, C–S or C–P bond is formed through the linkage of two fragments catalysed by a TM species, and constitute a powerful methodology in organic chemistry nowadays. One of the most important examples is the Heck reaction (or Mirozoki-Heck reaction, Scheme 3a),[22] which can be described as an olefin vinylation/arylation process employing an aryl/vinyl halide (or pseudohalide) with a large variety of alkenes in the presence of a palladium catalyst and a base. Another important class is the Sonogashira reaction (Scheme 3b),[23] which involves the formation of a new C–C bond between aryl or vinyl halides (or pseudohalides) and terminal acetylenes. This reaction is usually performed with a palladium catalyst, a copper (I) co-catalyst and a base. Although palladium is still the most used TM for the majority of cross-coupling reactions, in the last decades examples of Heck and Sonogashira reactions catalysed by other TM like nickel,[24] copper[25] or ruthenium,[26] among others, have been disclosed.

3. 1. 1. Heck reaction.

In 2014 Shafiee disclosed the first example of the Heck reaction catalysed by a graphenic material decorated with a transition metal complex acting as the active site.[27] Several other examples have been reported employing similar materials, which are shown in Figure 1. The above seminal work is based on a covalently anchored palladium complex, the material being labelled as Pd@AGu@MGO (**1**, Figure 1). To produce this new catalyst, GO was first decorated with homogeneously distributed Fe_3O_4 nanoparticles by co-precipitation of Fe(II) and Fe(III) giving the magnetic graphenic material labelled as MGO. Then, N-aminoguanidine was covalently linked to MGO surface by diethylene glycol moiety as organic spacer obtaining the aminoguanidine functionalized MGO. Finally, a five-membered chelate complex was formed by the reaction of the grafted N-aminoguanidine groups with $PdCl_2$ obtaining the final product Pd@AGu@MGO.

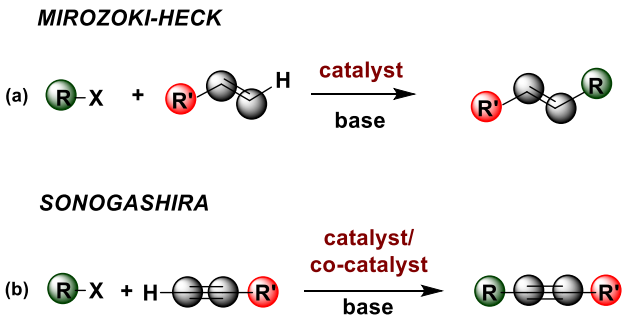

Scheme 3. The Mirozoki-Heck (a) and Sonogashira (b) reactions.

Shortly after the above report, Jia and Xi developed a novel palladium complex anchored on the surface of functional reduced graphene oxide (FRGO).[28] FRGO was synthetized through the reaction of GO and N-propylethane-1,2-diamine followed by the reduction with hydrazine hydrate. The as-prepared material contained nucleophilic terminal amine groups that can coordinate palladium by simple mixing of this material with $PdCl_2$, leading to Pd(II)–FRGO (**2**, Figure 1).

In 2016 Menendez reported the synthesis of a palladium complex covalently anchored onto thermally reduced graphene oxide, denoted as TRGO–NPy–Pd (**3**, Figure 1).[29] The catalyst precursor (TRGO–NPy) was prepared in few steps from thermally reduced GO (TRGO) employing well known diazonium chemistry[30] and simple organic reactions. Thus, an accessible nitrogen bidentate coordination site was generated in the graphene lattice. Finally, the palladium molecular complex $Pd(OAc)_2$ was covalently immobilized by reacting with TRGO–NPy obtaining the final catalyst TRGO–NPy–Pd.

Shaabani described a palladium complex supported on modified GO.[31] For the preparation of the catalyst, GO surface was first covalently modified by the reaction with keratin protein carrying amino,

hydroxyl, thiol and carboxyl groups. Then, Pd(II) tetrasulfophthalocyanine complex (PdTSPc) was covalently attached by condensation between the ligand sulphite groups and the amino groups in the mentioned grafted keratin protein, that acts as a linker among the support and the catalyst, giving the nanomaterial PdTSPc@KP–GO (**4**, Figure 1).

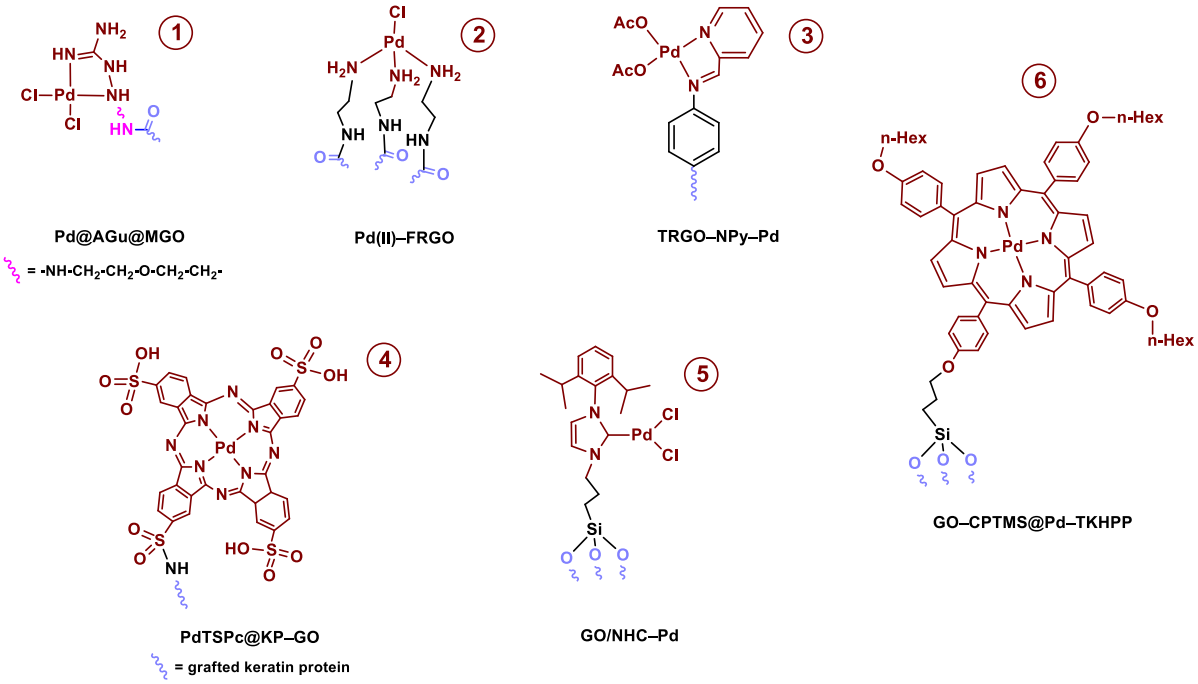

Figure 1. Graphene-supported catalysts employed in Heck-reactions. The graphenic material is not shown. Bluish color indicate linkers to surface.

In 2017 Shin and Lee developed a GO-supported NHC–Pd catalyst (denoted as GO/NHC–Pd; **5**, Figure 1).[32] To prepare the supported catalyst, the NHC precursor was covalently bonded on the GO surface via a silylation reaction, followed by chelation to $Pd(OAc)_2$. Nearly at the same time, Bahrami reported the synthesis of a Pd-porphyrin complex covalently supported on organosilane-functionalized GO.[33] The organosilane-functionalized GO (GO–CPTMS) was prepared by reaction between GO and CPTMS. Then, 5,10,15,20-tetrakis-(4-hexyloxyphenyl)-porphyrin was covalently anchored onto GO–CPTMS resulting in the GO–CPTMS@TKHPP material, before palladium is complexed yielding GO–CPTMS@Pd–TKHPP (**6**, Figure 1).

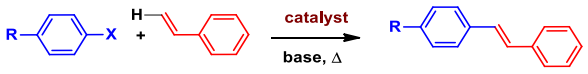

Scheme 4. Benchmark experiment for comparison of catalysts **1**-**6**.

The catalytic activity of those materials toward the Heck reaction is shown in Table 1, using as benchmark reaction that of bromobenzene (or iodobenzene) and styrene (Scheme 4). A range of yields within the interval 80-99% is reported for all catalysts, with the exception of **5** (55%). The nature of the substituent in the *para* position relative to the halide exerts a variable effect in the reaction outcome. Thus, catalysts **1** and **3** show no dependence of such groups, with yields being nearly identical for Me and NO_2 substituted arenes. The other four catalysts induce the Heck reaction with yields following the Me < H < NO_2 trend, the difference being more pronounced with catalyst **5**.

Table 1. Catalytic activity of **1**-**6** (Figure 1) for the Heck coupling of aryl arenes and styrene (Scheme 4).

Entry	Catalyst	X	R	Yield (%)	ref
1	**1**	Br	H	92	27
2	**1**	Br	4-NO_2	94	27
3	**1**	Br	4-Me	94	27
4	**2**	I	H	82	28
5	**2**	Br	4-NO_2	79	28
6	**2**	Br	4-OMe	66	28
7	**3**	Br	H	97	29
8	**3**	Br	4-NO_2	96	29
9	**3**	Br	4-OMe	94	29
10	**4**	Br	H	87	31
11	**4**	Br	4-NO_2	99	31**¡Error! Marcador no definido.**
12	**4**	Br	4-Me	80	31

Me < H < NO_2 trend, the difference being more pronounced with catalyst **5**.

The above activities are similar to a number of already described homogeneous catalysts for this transformation.[34] However, their solid nature, insoluble in all solvents, provides an additional and

convenient feature to their use, as their readily separation and potential reuse. Thus, catalysts **1**, **3** and **4** have been separated after the catalytic reaction and re-used, as shown in Figure 2. Catalyst **1** displayed the same catalytic activity after 10 runs, whereas eight and six reuses were reported for catalysts **3** and **4**, respectively, in which can be considered as the best improvement of these new

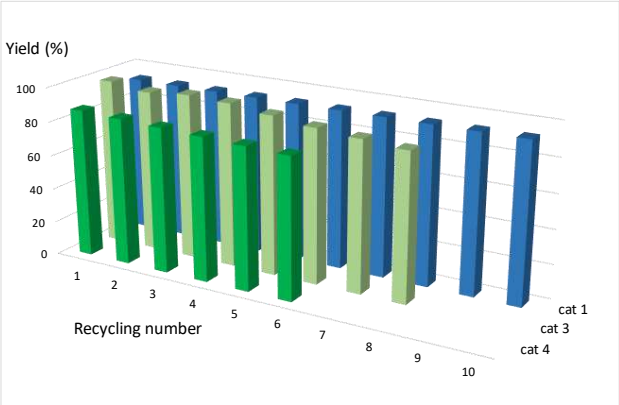

Figure 2. The recycling of catalysts **1**, **3** and **4** in Heck reactions. Bromobenzene employed in all cases, with styrene for catalysts **1** and **3**, and n-butyl acrylate for catalyst **4**.

materials from a catalytic point of view

3. 1. 2. Sonogashira reaction.

The coupling of aryl halides and terminal alkynes, the so-called Sonogashira reaction, was also induced by catalysts **4** and **5**, additionally to their performance in Heck reactions. Figure 3 displays three other examples reported in the literature for this same transformation. Hoseini synthesized a copper (I) complex covalently anchored onto organosilane-functionalized GO (**7**, Figure 3).[35] The functionalized GO was prepared by reaction between GO and 3 - aminopropyl)triethoxysilane (APTES). Then, the copper (I) complex was immobilized through ligand exchange reaction between one PPh_3 ligand of $[Cu(PPh_3)_3Cl]$ and the terminal amino group available on APTES-functionalized-GO yielding the material denoted as Cu(I)–f–GO.

Ghabdian reported a Cu(II) salen complex immobilized on GO (Cu(II)salen@GO, **8**, Figure 3). The Cu(II) salen complex was immobilized onto the GO support through an *in situ* strategy.[36] First, salen ligand was treated with CPTMS (chloropropyltrimethoxysilane) to generate $Si(OMe)_3$ anchoring sites. Then, $Cu(OAc)_2$ was added to prepare the metallic complex. Finally, the copper compound was mixed with GO affording the organosilane-linked Cu–GO catalyst.

Naeimi and co-workers prepared a Ni(II) complex covalently immobilized on GO (denoted as $GO@SiO_2$–BHEDNi, **9**, Figure 3).[37] The GO was first functionalized with chloropropyltrimethoxysilane (CPTMS) and treated with N,N'-bis(2-hydroxyethyl)ethylenediamine. Then, $NiCl_2$ was anchored onto the resulting material via covalent bonding between Ni and terminal hydroxy groups present in the functionalized GO.

Scheme 5 shows a general comparison of the catalysts described for Sonogashira reactions. Catalyst **4** provided yields varying from 33 to 99% with associated TON and TOF factors oscillating from 33 to 95 and from 3.66 to 10.55 h^{-1} respectively. Comparison with the unsupported palladium complex, PdTSPc@KP–GO exhibits better conversion with higher activity in the Sonogashira reactions of bromobenzene with phenylacetylene. In the case of catalyst **5**, it was used in different Sonogashira cross-coupling reactions in water employing CuI as co-catalyst and piperidine as base at 80 °C. Moderate yields ranging from 55 to 70% were obtained in the reaction of several aryl or heterocyclic halides with acetylene.

Catalyst **7** provided yields ranging from 69 to 97% in the reaction of different activated aryl iodides and bromides with phenylacetylene. As expected, the use of aryl chlorides led to lowers yields, ranging from 58 to 87%. For the mentioned reactions, TON and TOF factors are much higher than that for the unsupported complex. The supported catalyst exhibits TON and TOF values ranging from 1347 to 1979 and from 298 to 4241 h^{-1} respectively. The unsupported catalyst, in contrast, exhibits lowers TON and TOF factors, displaying values within the 43-69 and 5-80 h^{-1}

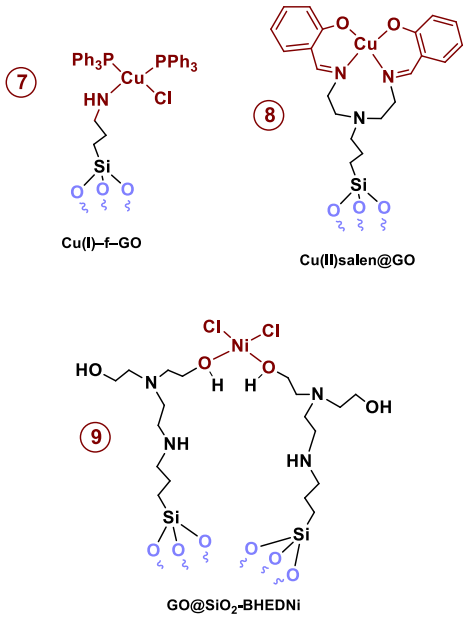

Figure 3. Graphene-supported catalysts employed in Sonogashira reactions.

intervals, respectively.

The Cu–GO material **8** was found to be active as catalyst in the Sonogashira reaction of several electronically diverse aryl halides with terminal acetylenes (yields = 65-98%; TON = 1857-2800) when a catalyst loading of 2.0 mol% was employed. This Cu–GO material exhibits a similar activity

towards the reaction of iodobenzene with phenylacetylene compared with that of unsupported Cu-salen complex.

In the case of catalyst **9**, yields ranging from 26 to 98% were obtained in the reaction of several structurally diverse aryl halides with phenylacetylene with TON and TOF values ranging from 9 to 34 and from 1.5 to 68 h^{-1}, respectively. This activity is higher in terms of yields, with shorter reaction times and milder reaction conditions, than previously reported Ni(II) homogeneous systems.

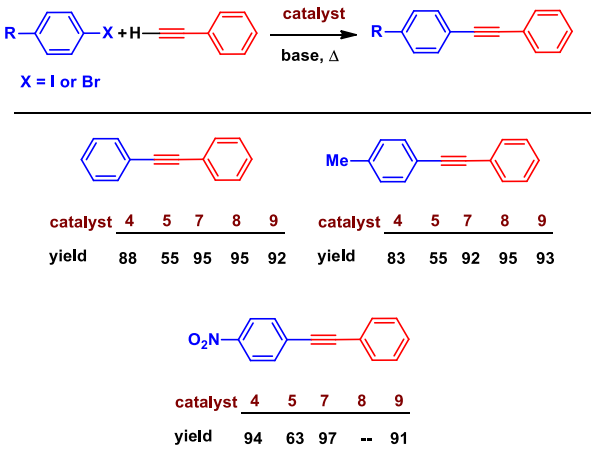

Scheme 5. Comparison of Sonogashira coupling reactions catalyzed by graphene-supported metal complexes.

Finally, the recyclability of these materials and further use in consecutive experiments must be commented. With the exception of **4**, all the materials were reported to maintain their catalytic properties upon separation from the final reaction mixture, washing and re-load of the reactants and solvents,

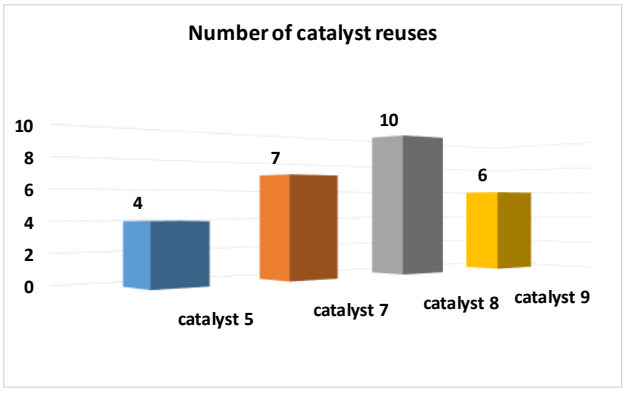

Figure 4. The recycling of catalysts **5** and **7-9** in-Sonogashira reactions.

with nearly no significant loss of activity (Figure 4). Catalyst **8** was employed up to ten times, whereas the other three materials could be recycled within the 4-7 range (Figure 4). This separation and reuse, along with the observance in most cases of a better performance when compared with the discrete, non-supported metal complex, make these materials good catalysts for this transformation.

3.1.3. Other cross-coupling reactions.

The already mentioned catalyst **2** (Figure 1) proved to be active in the Glaser homo-coupling reaction (Scheme 6).[28] Phenylacetylene or 1-octyne verified this transformation into diines, with a catalyst loading

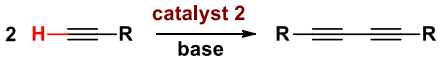

Scheme 6. Glaser homocoupling reaction.

of 0.5 mol% and CuI as co-catalyst, with yields of 98 and 95% respectively. To confirm the synergetic effect between Pd(II)–FRGO and CuI, similar reactions were carried out employing $PdCl_2$ instead of Pd(II)–FRGO. In these experiments the reactions did not take place, proving the good cooperation between both metals in this C–H functionalization process.

In addition to the graphene-supported catalysts described in the previous section for Heck or Sonogashira reactions, some others have been reported for other coupling reactions involving, at least, the activation of one C–H bond.

The synthesis of a heterogeneous Pd-catalyst covalently immobilized onto mesoporous silica/graphene surface, denoted as Pd@KIT–6/G–SH (**10**, Scheme 7) is due to Dabiri.[38] This nanohybrid material was found to be an active catalyst in two types of C–H functionalization reactions. First, it was tested in the ortho cyanation reaction of N-phenylacetamide derivatives employing a catalyst loading of 10 mol% and $K_4[Fe(CN)_6]$ as cyanide source with $Cu(OAc)_2$ (Scheme 7a). The cyanation of

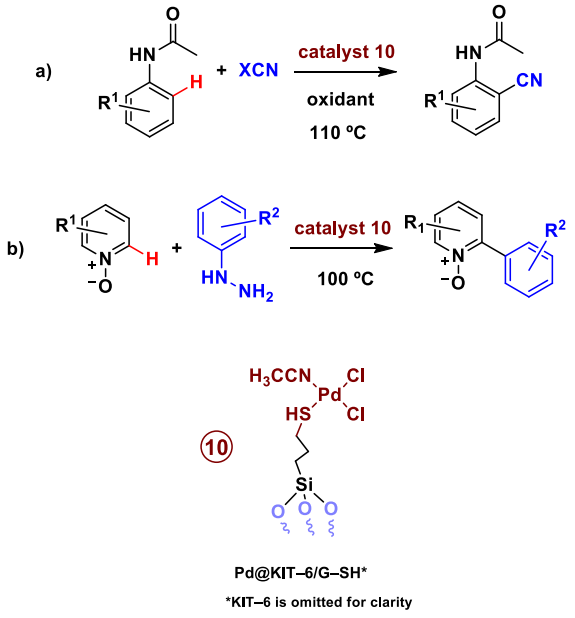

Scheme 7. a) Synthesis of 2-cyanoacetanilide derivatives and b) Preparation of arylpyridine derivatives with catalyst **10**.

acetanilide, chosen as model reaction, led to the formation of N-(2-cyanophenyl)acetamide in good yield (85%). The reaction was also carried out with a variety of electron-deficient and electron-rich acetanilide derivatives. Catalyst **10** was also examined as catalyst in the arylation of pyridine1-oxides with various arylhydrazine derivatives (Scheme 7b) under similar reaction conditions. A product yield of 74% was obtained in the reaction between pyridine-1-oxide and phenylhydrazine, chosen as model reaction. A further investigation of the reaction scope concludes that both pyridine-1-oxides bearing electron-donating and electron-withdrawing groups reacted well giving good yields.

The reusability of the Pd@KIT–6/G–SH **10** nanohybrid as catalyst for the cyanation of N-phenylacetamide with $K_4[Fe(CN)_6]$ was investigated. The catalyst was successfully recovered and reused over 7 cycles of reactions with a slight decrease in the catalytic activity from the initial value of 81 to 60%. TEM images of the recovered material showed the retained initial structure.

Shortly after, Blanco, Agnoli and co-workers disclosed the synthesis of both covalently ferrocene (Fc)-functionalized graphene acid (GA, a graphene material with a basal plane modified with COOH groups) and, for comparative purposes, covalently

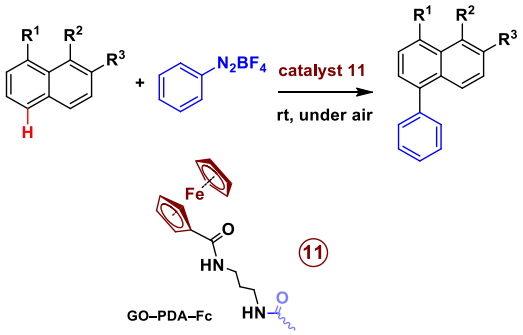

Scheme 8. C–H insertion of benzenediazonium tetrafluoroborate into several arene substrates with catalyst **11**.

Fc-functionalized graphene oxide (GO) nanosheets.[39] The catalytic activity of these materials (**11**, Scheme 8) was investigated in the arene C–H bond functionalization with diazonium salts employing 1.6 mol% of the heterogeneous catalyst and acetone as solvent at room temperature for 30 h under air. TON and turnover frequency at the beginning of the reaction (TOF^0) of 42 and 506.1 h^{-1} were respectively achieved employing GA–PDA–Fc as catalyst in the reaction between benzenediazonium tetrafluoroborate and naphthalene. At variance with that, the related GO–PDA–Fc gave lower TON and TOF values (32 and 134.0 h^{-1} respectively). Interestingly, the homogeneous molecular Fc catalyst performed similarly to the heterogeneous counterpart **11** (TON, 43; TOF^0 519.8 h^{-1}). The use of pyrene or anthracene demonstrated a better performance of **11**, compared with the GO-derivative or the molecular catalysts. In all cases, the reaction was selective to the insertion in the position 1 of the arene substrate. The reusability of both GA-based and GO-based material was tested in the reaction of benzenediazonium tetrafluoroborate with naphthalene. After 8 consecutive cycles no significant decrease in the catalytic activity of this catalyst was observed, thus manifesting its recyclability and durable catalytic performance.

A novel graphene oxide supported diimine-palladium complex (Pd–DI@GO, **12**, Scheme 9) was later reported by Li.[40] This catalyst was synthesized employing a covalent anchoring strategy and its catalytic performance was tested in C–H bond direct arylation reaction. Mono- and di-methylthiazoles were reacted with a variety of electron-rich and electron-deficient bromobenzenes (Scheme 9) employing a catalyst loading of **12** of 0.09 mol% under aerobic conditions. The reaction between 2,4-dimethylthiazole and bromobenzene, chosen as model reaction, afforded the product with a yield of 96%, substrate scope providing twenty-eight examples. Aryl bromides with neutral, electron-withdrawing, electron-donating or bulky groups can be effectively coupled with thiazole in excellent yields, which are comparable to the results obtained using homogeneous palladium catalysts. The formation of Pd(0) particles was confirmed by XRD analysis. A noticeable palladium leaching (14.5 wt%) was verified after performing several experiments direct arylation reactions, although experimental data showed that the reaction was catalysed by supported palladium and not soluble metal species. However,

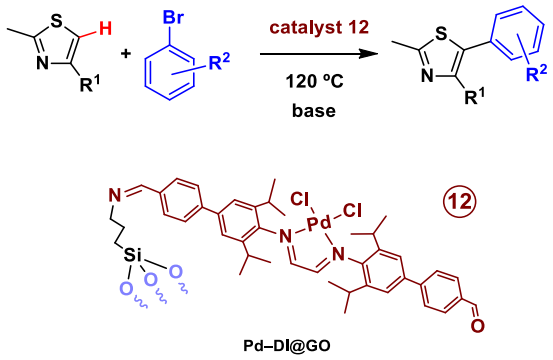

Scheme 9. Direct C–H bond arylation reaction of substituted thiazoles with catalyst **12**.

this leaching precluded catalyst recycling with good reusability.

Very recently, Heydari developed a novel palladium complex covalently supported on magnetic reduced graphene oxide, denoted as MRGO@DAP–AO–Pd(II) (**13**, Scheme 10),[41] containing Fe_3O_4 NPs. The catalytic activity of **13** was tested in the regioselective arylation of 1-methyl-1H-imidazole and 1,2-dimethyl-1H-imidazole with (hetero)aryl bromides (Scheme 10) employing a catalyst loading of 0.3 mol% in alkaline deep eutectic solvent (made of K_2CO_3 and glycerol in 1:5 ratio). In all

experiments, the C5-monoarylated imidazole was formed regioselectively, as C5 is more reactive than the C4 position in imidazoles. Excellent yield (95%) was obtained in the reaction between 1,2-dimethyl-1H-imidazole and 4-bromobenzaldehyde, chosen as the model reaction. Less-reactive aryl bromides bearing electron donating groups gave moderate yields of 64–75%, whereas sterically hindered 1-naphthyl bromide was prepared in 75% yield. Such reaction outcome was better than that previously reported with homogeneous palladium catalysts in C–H arylation reactions. Moreover, after 7 consecutive runs only a moderate deactivation of the catalyst was

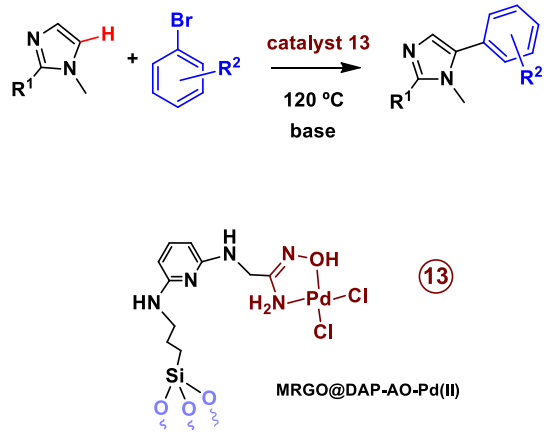

Scheme 10. Arylation reaction of imidazoles via C–H bond activation.

observed, with a decrease in the yields from 95 to 85%.

3. 2. Oxidation reactions.

Oxidation reactions are very useful synthetic tools in the chemical industry. The development of eco-friendly and recyclable systems has gained much interest,[42] the heterogenization of high active homogeneous catalytic systems being the most common strategy toward that end. To date, several graphene-supported catalysts have been reported for these transformations, showing the preferential use of base metals.

In 2013, Xiao reported the preparation of a cobalt(II)-salen complex (albeit the ligand does not correspond with the salen structure) covalently immobilized onto GO surface, labelled as Co–salen–GO (**14**, Scheme 11).[43] The catalytic performance of Co–salen–GO was tested in cyclohexene oxidation with a catalyst loading of 1.4 mol% and H_2O_2 as oxidant. A conversion of 21% was achieved with ca. 20% of selectivity toward cyclohexene epoxide. Even so, by-products derived from allylic C–H bond oxidation such as cyclohexen-2-ol and cyclohexen-2-one were observed with a total selectivity of 76%. In contrast, the Co-salen homogeneous catalyst displayed higher activity yielding cyclohexene conversion of 56% under the same reaction conditions. However, the selectivity into cyclohexene epoxide was only 3%. This catalyst can be reused 3 times with a low decrease (1%) on the cyclohexene conversion, indicating its excellent recyclability. Also,

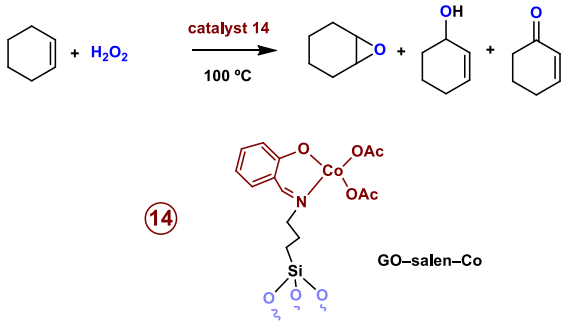

Scheme 11. Oxidation of cyclohexene with catalyst **14**.

the product distribution remains practically unchanged along the consecutive runs.

Huang has developed a protoporphyrinato iron (III) complex (known as Hemin) attached to modified graphene via non-covalent π-π interactions, and denoted as H–GN (**15**, Scheme 12).[44] This material was employed as catalyst in the oxidation of different saturated C–H bonds. For example, toluene was oxidized into mixtures of benzoic acid, benzaldehyde and benzylic alcohol (Scheme 12a), with long reaction times, a catalyst loading of 0.001 mol%, and using TBHP as initiator and oxygen as oxidant at 60 ºC. After 12 h a TON value of 9420 was measured. H–GN yields appreciably higher conversion rate (9.4%) than the soluble hemin (1%), explained as the result of hemin instability under oxidative conditions.[45] This fact reveals a protective function from the graphene support, that maintains hemin in the catalytically active form. Comparing with other systems, different selectivity was achieved employing H–GN as catalyst, a fact explained as a consequence

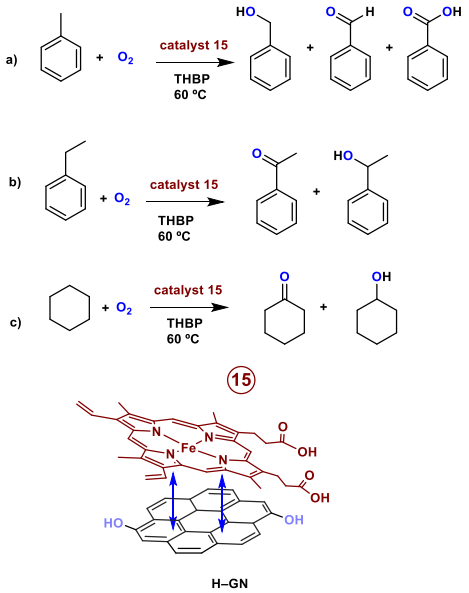

Scheme 12. Oxidation of several C–H bonds with catalyst **15** and O_2 as oxidant.

of graphene affecting the π-π interaction between the support and the substrate/oxidized products. The oxidation reactions of toluene, ethylbenzene and cyclohexane were carried out under optimized conditions. As expected, the conversion rate for ethylbenzene (12%) is higher than toluene, obtaining a ~5:4 mixture of acetophenone:phenylethanol (Scheme 12b). Cyclohexane (Scheme 12c) gave 8% conversion, after 12 h, providing cyclohexanone with a relative selectively of 57%.

A manganese(III)-porphyrin complex covalently supported onto GO nanosheets has been reported by Ravati.[46] The Mn-porphyrin complex was anchored to the GO surface by the ester bond formed between the hydroxyl group of the manganese complex and the carboxylic acid group of GO giving the graphenic nanocomposite Mn(THPP)OAc@GO (**16**, Scheme 13). When using indane as the substrate, only products derived from benzylic C–H oxidation were detected (17% indanone and 2% 1-indanole; Scheme 13a). The use of adamantane as aliphatic compound led to 92% of 1-adamantanol (Scheme 13c). The reusability of Mn(THPP)OAc@GO was tested for the aerobic oxidation of styrene under optimized conditions, with success, albeit no recycling was reported for C-H oxidation reactions.

Wendt have developed a NHC-palladium(II) complex non-covalently supported onto rGO surface (**17-rGO**, Scheme 14),[47] which was prepared by π-stacking support of the palladium complex onto the graphenic material. Catalyst **17-rGO** was employed in the undirected C–H acetoxylation of benzene (Scheme 14) with a catalyst loading of 0.3 mol% employing $PhI(OAc)_2$ as oxidant, providing a 50% yield of the desired product. The reactivity and

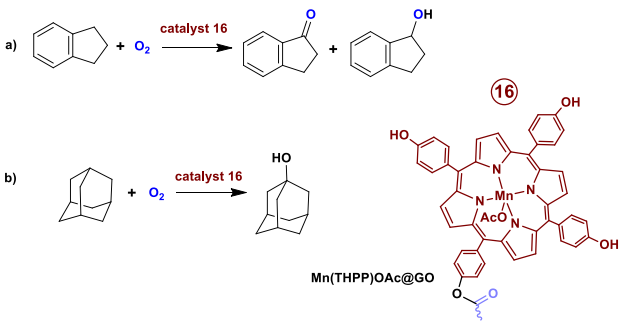

Scheme 13. Oxidation of indane (a), and adamantane (b) employing O_2 as oxidant and catalyst **16**.

regioselectivity of **17-rGO** were evaluated for the formation of acetoxylated products in toluene and biphenyl. A yield of 56% was obtained in the C–H acetoxylation of biphenyl with a product distribution of 39:47:14 for the para-, meta- and ortho-substituted positions respectively. The regioselectivity in the C–H acetoxylation of toluene is very low, with 38:33:29 for para-, meta- and ortho-substituted products displaying a total yield of 24%. These results show a catalytic efficiency in the supported material which is, at best, similar than that of the homogeneous analogue. The recyclability of this catalyst was tested in the acetoxylation of benzene. After 4 consecutive runs only a slight decrease of 4% in the product yield was observed, with a measurable Pd leaching of less than 0.011 ppm per cycle.

Very recently, Wang, Jiao and Liu have developed

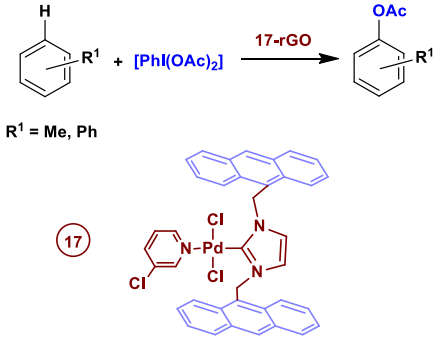

Scheme 14. C–H bond acetoxylation reaction of different arenes employing $PhI(OAc)_2$ as oxidant and catalyst **17-rGO**.

a phthalocyanine-Co(II) complex covalently anchored onto GO surface, denoted as CoAlPc/GO (**18**, Scheme 15).[48] This material exhibited a good activity for the photocatalytic degradation of phenol under visible light irradiation, a process which takes place via an o-benzoquinone intermediate (Scheme 15), which is strictly a product derived from the C–H bond oxidation on phenol. For a high (100 mg/L) phenol concentration and CoAlPc/GO dosage of 0.005 g, a degradation of 95% was achieved after 60

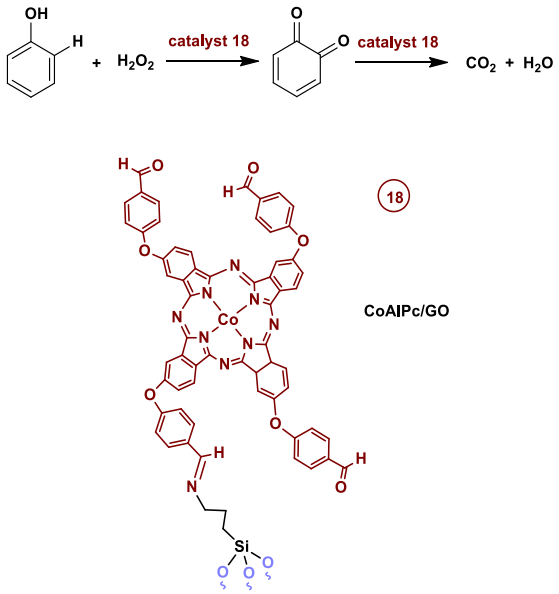

Scheme 15. Phenol photocatalytic degradation pathway with catalyst **18**.

min.

3. 3. Three-component reactions.

Several graphene-supported copper-based catalysts have also been employed to promote three component reactions, i. e., processes in which three different reactants are involved en route to the formation of one single product.

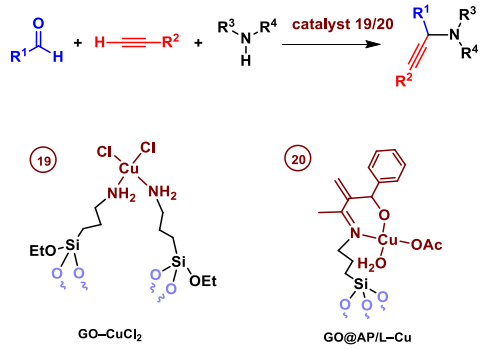

Scheme 16. The **19**/**20**-catalyzed aldehyde-alkyne-amine (A^3) reaction.

Xiong reported the synthesis of copper (II) complex covalently supported onto GO (GO–$CuCl_2$, **19**, Scheme 16)[49] as catalyst for the synthesis of propargylamines via one-pot multicomponent aldehyde-alkyne-amine coupling reaction (also known as A^3 reaction; Scheme 16). Yields ranged from good to excellent, including multi-gram scale. The reaction between benzaldehyde, phenylacetylene and morpholine, chosen as the model reaction, gave 96% of the desired product. This probe reaction also served to demonstrate the reusability of the catalysts, which was employed for five consecutive runs with no significant decrease in the catalytic activity. An array of aldehydes, alkynes and amines were reacted in the presence of **19** under microwave (MW) irradiation. The yields are comparable to those obtained using $CuCl_2$ and CuBr as catalysts, but providing the benefit of recycling. A scale-up experiment with formaldehyde, phenylacetylene and diethylamine with 150 mmol led to the product in 88% yield.

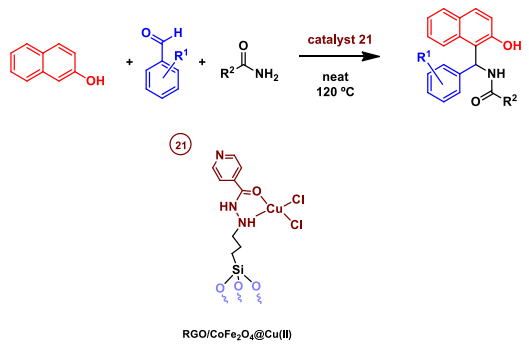

Scheme 17. Synthesis of substituted amidoalkylnaphthols catalyzed by **21**.

A second catalyst employed in the A^3 reaction was reported by Sharma,[50] consisting of a Cu(II)-Schiff base complex covalently immobilized onto GO surface, denoted as GO@AP/L - Cu (**20**, Scheme 16). High yields (~76-92%) were achieved, with water as the solvent. Recyclability was not studied with this reaction, but with the Chan-Lam coupling, for which five cycles were run without significant variation in activity.

Kooti and co-workers later prepared a Cu(II) complex covalently supported on magnetic reduced graphene oxide tagged as RGO/$CoFe_2O_4$@Cu(II) (**21**, Scheme 17).[51] The catalytic activity of this material

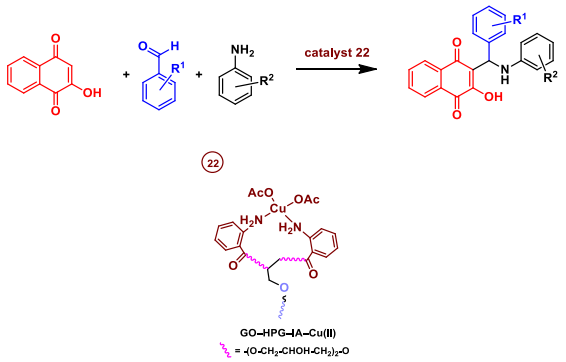

Scheme 18. Synthesis of aminonaphthoquinones catalyzed by **22**.

was investigated in the three-component one-pot condensation of aromatic aldehydes, 2-naphthol and amides for the synthesis of 1- amidoalkyl-2-naphthols derivatives employing 0.8 mol% of catalyst under solvent-free conditions at 120 °C, with yields within the range of 85-92% (Scheme 17). When compared with other catalytic systems, **21** exhibits a superior performance with lower reaction times and milder reaction conditions. Additionally, the magnetic nature of **21** provides an easy recovery from the reaction media, allowing up to five consecutive runs with the same activity and neglectable copper leaching.

Naeimi disclosed another copper (II) complex covalently immobilized onto hyperbranched polyglycerol (HPG) functionalized GO, labelled as GO-HPG-IA-Cu(II) (**22**, Scheme 18).[52] This material was tested as catalyst in the one-pot three-component reaction of 2-hydroxy-1,4-naphthoquinone with a variety of electron-rich and electron-deficient aldehydes and amines employing 0.1 mol% of catalyst (Scheme 18). The model reaction of 2-hydroxy-1,4-naphthoquinone, 4-chlorobenzaldehyde and 4-methoxyaniline originates the corresponding product in 95% yield, and TON and TOF values of 47 and 82 h^{-1} respectively. All substrates led to high yields (84-95%), which were, at least, similar, if not better, than a number of other catalysts employed for this transformation, with the added value of being recycled for five times without loss of activity.

3. 4. Miscellaneous reactions.

In this section several transformations that cannot be included in the previous classifications are discussed.

In 2014 Fan and co-workers reported the synthesis of a tertiary organic amine and palladium-diamine complex simultaneously immobilized, in a covalent manner, on GO support, and denoted as GO–NEt_2–2N–Pd (**23**, Scheme 19).[53] This novel nanocomposite was found to be an active and reusable catalyst for the Tsuji–Trost allylation.[54] This reaction requires the presence of both a metallic active site and a base that promotes the activation of the nucleophile to attack the metalated intermediate species in the catalytic cycle. Employing allyl methyl carbonate and ethyl acetoacetate (Scheme 19) and a catalyst loading of 0.4 mol%, the transformation proceeded with yields of 88% for the mono-allylation product and 4% for the di-allylation product, with a

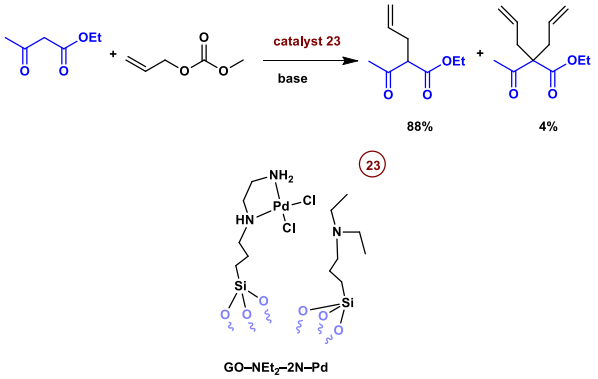

Scheme 19. The Tsuji–Trost allylation of allyl methyl carbonate with ethyl acetoacetate catalyzed by **23**.

final TOF of 46 h^{-1}. The amine-free catalyst (denoted as GO–2N–Pd) was synthetized for comparative purposes, its catalytic activity being half of that of **23** under the same conditions. The latter could be reused for five consecutive cycles with no significant decrease in the catalytic activity. The excellent performance was explained in terms of the synergistic catalysis effect, excellent support properties, and robust immobilization interaction.

In 2015, Peris described the preparation of a series of pyrene-tagged N-heterocyclic carbene complexes of iridium and their rGO non-covalently supported homologues.[55] These new catalysts were tested in the reduction of ketones by transfer hydrogenation and in the β-alkylation of secondary alcohols with primary alcohols. Iridium-NHC complexes bearing one pyrene tags were both supported onto reduced graphene oxide (rGO) by simple mixing of the molecular complexes with rGO, affording the solids **24-rGO** and **25-rGO** (Scheme 20). The catalytic properties of both materials were tested in the β-alkylation of 1-phenylethanol with benzyl alcohol (Scheme 20), employing a catalyst loading of 0.5 mol%. The yields were moderate for **24-rGO** and high for **25-rGO**. The same pattern was found when studying the recyclability, **25-rGO** could be recycled 12 times without loss of activity whereas **24-rGO** exhibits a gradual loss of activity until complete deactivation on the 7th run, probably due to a faster desorption, in line with ICP-MS analysis after the recycling experiments. It is worth noting that both catalysts exhibit slightly enhanced performance in the first few recycling runs when compared with the fresh materials. This behaviour is consequence of the need of activation of both catalysts along the reaction course, as verified by kinetics studies of the reaction

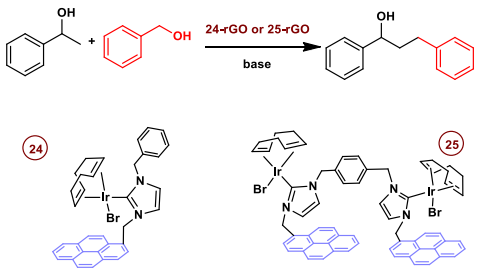

Scheme 20. β-Alkylation of 1-phenylethanol with benzyl alcohol catalyzed by **24-rGO** or **25-rGO**.

profiles.

Finally, in our first contribution to this field, in collaboration with the group of Mata, we have investigated the catalytic properties of a copper complex bearing an N-heterocyclic carbene ligand with a pyrene tag, both molecularly and non-covalently immobilized onto rGO (**26-rGO**, Scheme 21)[56] in the carbon-hydrogen bond functionalization by carbene insertion from ethyl diazoacetate, EDA (Scheme 21). The comparison of the homogeneous and heterogeneous catalysts was carried out using n-hexane, cyclohexane and benzene as substrates in reactions involving the transfer of the $CHCO_2Et$ group from EDA, employing a catalyst loading of 1.0 mol% and $NaBAr^F_4$ as halide scavenger. Catalyst **26-**

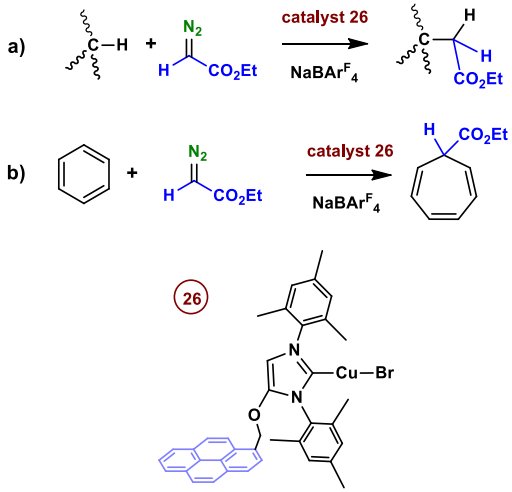

Scheme 21. C–H functionalization by carbene insertion from a diazo compound catalyzed by **26-rGO**.

rGO afforded the products derived from the carbene insertion in the C–H bonds for cyclohexane and n-hexane (Scheme 21a) in moderate yields (34 and 38% respectively), whereas for benzene only the product derived from the addition to the double bond in the so-called Buchner reaction (Scheme 21b)[57] was obtained in 37% of yield. Albeit the conversions are

moderate, this behaviour surpasses that of the homogeneous system, i. e. the molecular copper complex **26**: 15% for cyclohexane, 16% for n-hexane and 10% for benzene. Thus, a beneficial effect of the support is observed in this transformation (vide infra). It is worth noting that EDA was not completely consumed even after stirring for 4 days at room temperature. The existence of a deactivation process affecting the metal centre in a similar way for the homogeneous and heterogeneous system was proposed, since filtration tests indicated the absence of significant copper leaching from the support.

4. The role of graphenic supports

The heterogeneous nature of the materials included in this contribution provides one immediate advantage to their use: a readily catalyst separation and, in many cases, reuse for a number of subsequent cycles. Two questions frequently arise when dealing with heterogeneous catalysts generated from the anchoring of a homogenous catalyst on a support and referred to the latter. One is related to the possible deterioration of the support, which may be an indication of secondary reactions, usually non-desired from a catalytic point of view. The other is about the role of the support, whether it acts as spectator or as a non-innocent partner.

4.1. Graphene-material deterioration during catalysts.

Reports contained in this review provide distinct information with respect to the above questions. A number of them do not include experimental data related to the role of the support or its stability, despite their use at high temperatures in many cases. Other reports have compared spectroscopic (FTIR, UV-Vis) or microscopy (SEM, TEM, XPS) data of the solid catalyst before and after catalysis, or after each cycle. It is worth noting that in most of those cases no significant changes were observed, demonstrating the stability of the graphene-modified solids during catalysis for different transformations and reaction conditions. Graphene oxide, in any of their variants (GO, rGO, TRGO, MRGO) was the support which remains unaltered in the case of catalysts **3**,[29] **5**,[32] **11**[39] and **13**[41] for cross-coupling reactions; **18**[48] for C-H bond oxidation, **19**,[49] **21**[51] and **22**[52] for three-component reactions, **23**[53] for allylation reaction and **26-rGO**[56] for carbene insertion into C-H bonds. There is only one exception, that of catalyst Pd–DI@GO (**12**)[40] for which studies carried out by SEM demonstrated that the morphology of the GO changed during catalysis, affecting the agglomeration of the GO layers. However, we must note that such modification was observed during its use in Suzuki reactions, not included in this review.

4.2. Role of the graphene-material in the catalytic outcome.

The second question relative to the role of the support within the catalytic reaction which induces, in many cases, an enhancement of the catalytic activity, has been only explained in several articles included in this contribution, and not always with the support of experimental data. However, there are some of them that have shed light to this effect which, in principle, could be applied to the other examples. The following are the main reasons argued to account for such behaviour, which could occur simultaneously in a given catalytic system:

a) Layers and surface area. The fact that the graphene-derived supports display two dimensional structures with high surface areas sustains the lack of mass transfer resistance, the reactants and the products readily reaching/leaving the catalytic active sites.[29,33,35,44,53]

b) Separation of active sites. In many occasion, homogeneous catalysts deactivate upon formation of aggregates or nanoparticulate materials. Their fixation at these layered materials precludes their approach and further decomposition. Also, these materials are prone to fix nanoparticles, maintaining the solution somewhat clean of such agglomerates which can also produce side reactions.[29,40,44]

c) Interactions of the support with aromatic reagents. The existence of π-π interactions between the graphene material and the aromatic reactants has been invoked in several cases to explain a better catalytic performance. It is assumed that such interaction activates the ring as well as it approaches it to the active site. [31,39,44,55]

d) Electronic modification of the metal center. In some cases, with non-covalent interactions, it has been proposed that a next flux of electronic density takes place from the metal complex to the graphene surface, such as in catalysts CoAIPc/GO (**18**) or **26-rGO**. Such electronic transfer positively affects the catalytic reaction in such a way that enhances the reaction outcome.[48,56]

5. Conclusions

In the context of heterogeneous catalysis, the use of carbon-based layered materials as support for transition metal catalysts such as graphene provides several advantages compared with traditional supports. In this contribution the application of graphene materials, in different forms, to catalytic processes involving the functionalization of a carbon-hydrogen bond of one of the reactants has been reviewed. In most of the examples included, the catalytic properties of the heterogeneous materials include better yields, TON and/or TOF than other catalysts in traditional supports or than the homogeneous counterpart. Such behaviour can be explained because of two effects. On one hand, these

materials do not show pores or irregular surfaces, where catalytic centres could be less active; on the other hand, the planar structure facilitates the linkage to the catalyst moiety in a very similar manner for all the active centres. Secondly, in some cases the surface contributes to activate either the catalyst or the substrate, due to the capabilities of the graphene material to interact and affect electronic properties. Given the current trend toward sustainable catalysis, which requires easy separation and recycling, the use of graphene-based heterogeneous materials emerges as an excellent alternative to traditional supports. The expansion of this strategy to many catalytic transformations is yet to be developed.

Acknowledgements

Support for this work was provided by the MINECO (CTQ2017-82893-C2-1-R, Junta de Andalucía (P18-RT-1536) and PO FEDER 2014-2020, UHU-1260216). JM thanks MINECO for a FPI fellowship.

References

[1] a) P. W. N. M. van Leeuwen in *Homogeneous Catalysis: Understanding the art*, Springer, Netherlands, **2004**; b) P. W. N. M. van Leeuwen, J. C. Chadwick in *Homogeneous Catalysts: Activity - Stability – Deactivation*, Wiley-VCH, Weinheim, **2011**.

[2] a) Y. Yermakov, V. Likholobov in *Homogeneous and Heterogeneous Catalysis: Proceedings of the Fifth International Symposium on Relations Between Homogeneous and Heterogeneous Catalysis*, VNU Science Press, Netherlands, **1986**; b) L. Can, L. Yan, in *Bridging Heterogeneous and Homogeneous Catalysis: Concepts, Strategies, and Applications*, Wiley-VCH, Weinheim, **2014**.

[3] C. Collis, T. Horvath, *Catal. Sci. Technol.* **2011**, *1*, 912-919.

[4] See, for example: a) P. McMorn, G. J. Hutchings, *Chem. Soc. Rev.* **2004**, *33*, 108–112; b) J. M. Fraile, J. I. García, J. A. Mayoral, *Chem. Rev.* **2009**, *109*, 360–417.

[5] A. Thrower in *Chemistry & Physics of Carbon*, *Vol. 25*, CRC Press, **1996**.

[6] K. S. Novoselov, A. K. Geim, S. V. Morozov, D. Jiang, Y. Zhang, S. V. Dubonos, I. V. Grigorieva, A. A. Firsov, *Science* **2004**, *306*, 666–669.

[7] a) M. R. Axet, J. Durand, M. Gouygou, P. Serp, *Adv. Organomet. Chem.* **2019**, *71*, 53-174.; b) E. M. Pérez, N. Martín, *Chem. Soc. Rev.* **2015**, *44*, 6425–6433.

[8] a) B. I. Kharisov, O. V. Kharissova, A. Vázquez Dimas, I. Gómez De La Fuente, Y. Peña Méndez, *J. Coord. Chem.* **2016**, *69*, 1125–1151; b) S. Navalón, J. R. Herance, M. Álvaro, H. García, *Chem. Eur. J.* **2017**, *23*, 15244–15275; c) V. Campisciano, M. Gruttadauria, F. Giacalone, *ChemCatChem* **2019**, *11*, 90–133.

[9] N. M. Julkapli, S. Bagheri, *Int. J. Hydrog. Energy.* **2015**, *40*, 948–979.

[10] F. Bonaccorso, L. Colombo, G. Yu, M. Stoller, V. Tozzini, A. C. Ferrari, R. S. Ruoff, V. Pellegrini, *Science* **2015**, *347*, 1246501.

[11] Y. Chen, C. L. Tan, H. Zhang, L. Z. Wang, *Chem. Soc. Rev.* **2015**, *44*, 2681–2701.

[12] a) V. Georgakilas, J. N. Tiwari, K. C. Kemp, *Chem Rev.* **2016**, *116*, 5464–5519; b) A. Eftekhari, H. Garcia, *Mater. Today Chem*. **2017**, *4*, 1–16.

[13] a) Y. Xu, H. Bai, G. Lu, C. Li, G. Shi, *J. Am. Chem. Soc*. **2008**, *130*, 5856–5857; b) W. Yang, H. Grennberg, *ECS Transactions* **2009**, *19*, 3975–3983.

[14] a) S. Sakthinathan, H. F. Lee, S.-M. Chen, P. Tamizhdurai, *J. Colloid Interface Sci.* **2016**, *468*, 120–127; b) D. Ventura-Espinosa, C. Vicent, M. Baya, J. Mata, *Catal. Sci. Technol.* **2016**, *22*, 8024–8035; c) J. S. Lee, S. H. Lee, J. Kim, C. B. Park, *J. Mater. Chem. A*. **2013**, *1*, 1040–1044; d) L. Zhang, E. Yue, B. Liu, *Catal. Commun.* **2014**, *43*, 227–230; e) B. Choi, J. Lee, S. Lee, *Macromol. Rapid Commun.* **2013**, *34*, 533–538.

[15] a) J. A. Mann, J. Rodríguez-López, H. D. Abruna, W. R. Dichtel, *J. Am. Chem. Soc.* **2011**, *133*, 17614–17617; b) M. Keller, V. Colliere, O. Reiser, A.-M. Caminade, J.-P. Majoral, A. Ouali, *Angew. Chem. Int. Ed.* **2013**, *52*, 3626–3629.

[16] L. Sung, *Chin. J. Chem. Eng.* **2019**, *27*, 2251–2260.

[17] a) A. T. Smith, A. M. LaChance, S. Zeng, B. Liu, L. Sun, *Nano Materials Sci.* **2019**, *1*, 31–47; b) T. Kuilla, S. Bhadra, D. Yao, N. H. Kim, S. Bose, J. H. Lee, *Prog. Polym. Sci.* **2010**, *35*, 1350–1375.

[18] a) Q. Zhao, Y. Li, R. Liu, A. Chen, G. Zhang, F. Zhang, X. Fan, *J. Mater. Chem. A* **2013**, *1*, 15039–15045; b) Q. Zhao, D. Chen, Y. Li, G. Zhang, F. Zhang, X. Fan, *Nanoscale* **2013**, *5*, 882–885; c) Z. Li, S. Wu, D. Zheng, H. Liua, J. Hu, H. Su, J. Sun, X. Wang, Q. Huo, J. Guan, K. Kan, *Appl. Catal. A* **2014**, *470*, 104–114; d) P. K. Khatri, S. C. Choudhary, R. Singh, S. L. Jain, O. P. Khatri, *Dalton Trans.* **2014**, *43*, 8054–8061.

[19] a) M. J. McAllister, J.-L. Li, D. H. Adamson, H. C. Schniepp, A. A. Abdala, J. Liu, M. Herrera-Alonso, D. L. Milius, R. Car, R. K. Prudhomme, *Chem. Mater.* **2007**, *19*, 4396–4404; b) H. C. Schniepp, J.-L. Li, M. J. McAllister, H. Sai, M. Herrera-Alonso, D. H. Adamson, R. K. Prudhomme, R. Car, D. A. Saville, I. A. Aksay, *J. Phys. Chem.* **2006**, *110*, 8535–8539; c) A. Kaniyoor, T. T. Baby, S. Ramaprabhu, *J. Mater. Chem*. **2010**, *20*, 8467–8469; d) M. Zhou, Y. Wang, Y. Zhai, J. Zhai, W. Ren, F. Wang, S. Dong, *Chem. Eur. J.* **2009**, *15*, 6116–6120; e) D. R. Dreyer, S. Park, C. W. Bielawski, R. S. Ruoff, *Chem. Soc. Rev.* **2010**, *39*, 228–240; f) C. A. Amarnath, C. E. Hong, N. H. Kim, B.-C. Ku, T. Kuila, J.-H. Lee, *Carbon* **2011**, *49*, 3497–3502; g) J. Liu, J. Tang, J. J. Gooding, *J. Mater. Chem.* **2012**, *22*, 12435–12452; h) S. Pei, H.-M. Cheng, *Carbon* **2012**, *50*, 3210–3228; i) Y. Liu, Y. Zhang, G. Ma, Z. Wang, K. Liu, H. Liu, *Electrochimica Acta* **2013**, *88*, 519–525.

[20] a) A. Das, B. Chakraborty, A. K. Sood, *Bull. Mater. Sci.* **2008**, *31*, 579–584; b) D. Graf, F. Molitor, K.

Ensslin, C. Stampfer, A. Jungen, C. Hierold, L. Wirtz, *Nano Lett.* **2007**, *7*, 238–242.
[21] a) F. Diederich, P. J. Stang in *Metal-Catalyzed Cross-Coupling Reactions*, Wiley-VCH, **1998**; b) N. Miyaura in *Cross-Coupling Reactions: A Practical Guide*, Springer, **2002**.
[22] a) R. F. Heck, J. P. Nolley, *J. Org. Chem.* **1972**, *37*, 2320–2322; b) T. Mizoroki, K. Mori, A. Ozaki, *Bull. Chem. Soc. Jpn.* **1971**, *44*, 581.
[23] K. Sonogashira, Y. Tohda, N. Hagihara, *Tetrahedron Lett.* **1975**, *16*, 4467–4470.
[24] a) M. R. Kwiatkowski, E. J. Alexanian, *Angew.Chem. Int. Ed.* **2018**, *57*, 16857–16860; b) J. Yi, X. Lu, Y. Sun, B. Xiao, L. Liu, *Angew. Chem. Int. Ed.* **2013**, *52*, 12409 –12413.
[25] a) Y. Peng, J. Chen, J. Ding, M. Liu, W. Gao, H. Wu, *Synthesis* **2011**, *2*, 213-216; b) F. Monnier, F. Turtaut, L. Duroure, M. Taillefer, *Org. Lett.* **2008**, *10*, 3203–3206.
[26] a) J. M. Muñoz-Molina, P. J. Pérez, *J. Org. Chem.* **2019**, *84*, 8289–8296; b) S. Park, M. Kim, D. H. Koo, S. Chang, *Adv. Synth. Catal.* **2004**, *346*, 1638–1640.
[27] L. Ma'mani, S. Miri, M. Mahdavi, S. Bahadorikhalili, E. Lotfi, A. Foroumadia, A. Shafiee, *RSC Adv.* **2014**, *4*, 48613–48620.
[28] S. Wang, D. Hu, W. Hua, J. Gu, Q. Zhang, X. Jia, K. Xi, *RSC Adv.* **2015**, *5*, 53935–53939.
[29] L. Fernández-García, M. Blanco, C. Blanco, P. Álvarez, M. Granda, R. Santamaría, R. Menéndez, *J. Mol. Cat. A: Chem.* **2016**, *416*, 140–146.
[30] A. Schaetz, M. Zeltner, W. Stark, *ACS Catal.* **2012**, *2*, 1267–1284.
[31] Z. Hezarkhani, A. Shaabani, *RSC Adv.* **2016**, *6*, 98956–98967.
[32] S. Kim, H. Cho, D. Shin, S. Lee, *Tetrahedron Lett.* **2017**, *58*, 2421–2425.
[33] K. Bahrami, S. N. Kamrani, *Appl. Organomet. Chem.* **2018**, *32*, 4102–4111.
[34] a) S. Jagtap, *Catalysts* **2017**, *7*, 267; b) I. P. Beletskaya, A. V. Cheprakov, *Chem. Rev.* **2000**, *100*, 3009−3066.
[35] R. H. Fath, S. J. Hoseini, *Appl. Organomet. Chem.* **2018**, *32*, 3964–3972.
[36] M. Ghabdian, M. A. Nasseri, A. Allahresani, A. Motavallizadehkakhky, *Appl. Organomet. Chem.* **2018**, *32*, 4545–4553.
[37] H. Naeimi, F. Kiani, *J. Organomet. Chem.* **2019**, *885*, 65–72.
[38] M. Dabiri, S. I. Alavioon, S. K. Movahed, *ChemistrySelect* **2018**, *3*, 3487–3494.
[39] D. Mosconi, M. Blanco, T. Gatti, L. Calvillo, M. Otyepka, A. Bakandritsos, E. Menna, S. Agnoli, G. Granozzi, *Carbon* **2019**, *143*, 318–328.
[40] Y. Sun, T. Li, *ChemistrySelect* **2020**, *5*, 1431-1438.
[41] M. Shariatipour, A. Salamatmanesh, M. J. Nejad, A. Heydari, *Catal. Commun.* **2020**, *135*, 105890.
[42] F. Cavani, *Catal. Today* **2010**, *157*, 8–15.
[43] J. Sun, J. Zhang, L. Wang, L. Zhu, X. Meng, F.-S. Xiao, *J. Energy Chem.* **2013**, *22*, 48–51.
[44] Y. Li, X. Huang, Y. Li, Y. Xu, Y. Wang, E. Zhu, X. Duan, Y. Huang, *Sci. Rep.* **2013**, *3*, 1–7.
[45] a) B. Meunier, *Chem. Rev.* **1992**, *92*, 1411–1456; b) C. K. Chang, M. Kuo, *J. Am. Chem. Soc.* **1979**, *101*, 3413–3415; c) R. D. Arasasingham, A. L. Balch, C. R. Cornman, L. Latos-Grazynski, *J. Am. Chem. Soc.* **1989**, *111*, 4357–4363.
[46] S. Rayati, S. Rezaie, F. Nejabat, *C. R. Chim.* **2018**, *21*, 696–703.
[47] a) M. H. Majeed, P. Shayesteh, A. R. Persson, L. R. Wallenberg, J. Schnadt, O. F. Wendt, *Eur. J. Inorg. Chem.* **2018**, 4742–4746; b) N. Yuan, M. H. Majeed, E. G. Bajnóczi, A. R. Persson, L. R. Wallenberg, A. K. Inge, N. Heidenreich, N. Stock, X. Zou, O. F. Wendt, I. Persson, *Catal. Sci. Technol.* **2019**, *9*, 2025–2031.
[48] Y. Liu, P. Zuo, F. Wang, J. Men, R. Wang, W. Jiao, Y. Liu, *J. Taiwan Inst. Chem. Eng.* **2019**, *104*, 187–200.
[49] X. Xiong, H. Chen, R. Zhu, *Catal. Commun.* **2014**, *54*, 94–99.
[50] A. Mittal, S. Kumari, Parmanand, D. Yadav, S. K. Sharma, *Appl. Organomet. Chem.* **2020**, *34*, 1–12.
[51] M. Kooti, M. Karimi, E. Nasiri, *J. Nanopart. Res.* **2018**, *20*, 1–16.
[52] H. Naeimi, M. F. Zarabi, *Tetrahedron* **2018**, *74*, 2314–2323.
[53] Q. Zhao, Y. Zhu, Z. Sun, Y. Li, G. Zhang, F. Zhang, X. Fan, *J. Mater. Chem. A* **2015**, *3*, 2609–2616.
[54] a) J. Tsuji, H. Takahashi, M. Morikawa, *Tetrahedron Lett.* **1965**, *6*, 4387-4388; b) B. M. Trost, T. J. Fullerton, *J. Am. Chem. Soc.* **1973**, *95*, 292–294.
[55] S. Ruiz-Botella, E. Peris, *Chem. Eur. J.* **2015**, *21*, 15263–15271.
[56] P. Ballestin, D. Ventura-Espinosa, S. Martin, A. Caballero, J. A. Mata, P. J. Pérez, *Chem. Eur. J.* **2019**, *25*, 9534–9539.
[57] E. Buchner, T. Curtius, *Ber. Dtsch. Chem. Ges.* **1885**, *18*, 2371–2377.

FULL PAPER

Graphene-Supported, Well-Defined Metal-Based Catalysts for C-H Bond Functionalization and Related Reactions

Adv. Synth. Catal. **Year**, *Volume*, Page – Page

Jonathan Martínez-Laguna,[a] Ana Caballero*,[a] and Pedro J. Pérez*,[a]